Journal of Alloys and Compounds 488 (2009) 238–242

Contents lists available at ScienceDirect

Journal of Alloys and Compounds

journal homepage: www.elsevier.com/locate/jallcom

Mechanically activated self-propagating high-temperature synthesis of $La_{0.9}Sr_{0.1}Ga_{0.8}Mg_{0.2}O_{3-\delta}$ as an electrolyte for SOFC

Hiroyuki Ishikawa[a,1], Makiko Enoki[b], Tatsumi Ishihara[b], Tomohiro Akiyama[a,*]

[a] Center for Advanced Research of Energy Conversion Materials, Hokkaido University, Kita 13 Nishi 8, Kita-ku, Sapporo 060-8628, Japan
[b] Department of Applied Chemistry, Faculty of Engineering, Kyusyu University, Fukuoka 812-8581, Japan

ARTICLE INFO

Article history:
Received 24 March 2006
Received in revised form 21 August 2009
Accepted 22 August 2009
Available online 27 August 2009

Keywords:
Combustion synthesis
Lanthanum gallate
Solid oxide fuel cell (SOFC)
High-energy ball milling
X-ray diffraction

ABSTRACT

In this paper, we report on synthesis of highly pure $La_{0.9}Sr_{0.1}Ga_{0.8}Mg_{0.2}O_{3-\delta}$ (LSGM9182) powder with high crystallinity by mechanically activated (MA) self-propagating high-temperature synthesis (SHS), in which the synergy effects of MA and SHS on final and intermediate products were mainly examined. In the experiments, raw materials of La_2O_3, $SrCO_3$, Ga_2O_3, Mg and $NaClO_4$ were fractured and well mixed by planetary ball milling for different periods from 0 h to 24 h, then the bottom surface of the green compacts were electrically ignited for producing pure LSGM9182 through the propagation of sustainable exothermic reaction. The final and intermediate products, shortly after MA treatment, were characterized by XRD, SEM, XRF and particle size analyzer. During the planetary ball milling, the raw materials became gradually amorphous due to disordering of crystal structure. Interestingly, the longer milling operation caused the larger particle size of the raw material because nanoparticles, generated by the milling, became easily massed together. More significantly, the MA pretreatment improved a reactivity of the SHS to purify the product. In particular, the combination of MA–SHS with ball milling of 24 h at 300 rpm gave the highest-grade LSGM9182 product of nano-sized primary particles. The results appealed that the SHS after the MA treatment was quite effective for initiating, activating, sustaining and completing the solid–solid reaction synthesis of functional perovskite-type oxide with mild exothermic heat.

1. Introduction

Strontium- and magnesium-doped lanthanum gallate, $La_{1-x}Sr_xGa_{1-y}Mg_yO_{3-\delta}$ (LSGM), has attracted worldwide attention as a promising electrolyte material for solid oxide fuel cell (SOFC) at intermediate temperature around 873–1073 K. In particular, it was reported that *$La_{0.9}Sr_{0.1}Ga_{0.8}Mg_{0.2}O_{3-\delta}$ (LSGM9182)* exhibits large electrically conductivity, 0.1–0.15 S cm^{-1} at 1073 K, over a wide range of oxygen partial pressures (10^{-22}–1 atm) [1–3]. The production method of the LSGM9182 electrolyte is usually a conventional solid-state reaction method (SRM), which consists of a calcination step at 1273 K for 6 h and a sintering one at 1773 K for 6 h [1,2]. This is a relatively easy and reliable way for synthesizing the LSGM9182 bulk-material, but really time- and energy-consuming. In our previous study, we successfully produced the LSGM electrolyte by using *self-propagating high-temperature synthesis (SHS)* as an alternative method instead of the SRM [4,5]. This offers many benefits for utilizing exothermic heat of solid-phase reaction, omitting external energy, simplifying manufacturing equipments and minimizing processing time. However, the product was not a single phase of LSGM, requiring successive sintering treatment for producing the pure LSGM.

In practice, the commercial SOFC needs a thin-film electrolyte with large ratio of area/thickness to reduce the ohmic loss, generally produced by using thin-film fabrication technologies such as tape-casting and doctor blade method [6,7]. In this process, highly pure and fine powders are required to produce the high-quality ceramic membrane. However, it is difficult to provide the high-grade ones by the traditional SRM and SHS at present. Thus, many efforts have been continued by several groups to obtain the fine LSGM9182 powders using another synthetic routes such as sol–gel process, Pechini method [8,9] and glycine–nitrate combustion method [10–12]; these wet chemical syntheses are attractive in lowering the sintering temperature due to the size reduction of particle generated. Unfortunately, the powders with high crystallinity were not directly provided from the processes above mentioned, because the obtained ones were amorphous. In addition, these methods always requested expensive starting materials, such as metal alkoxides and nitrates, which were produced by time- and energy-consuming process. It was enough for motivating us to produce the highly pure LSGM9182 powders with high crystallinity by an alternative process, *mechanically activated self-propagating high-temperature synthesis (MASHS)*.

* Corresponding author. Tel.: +81 11 706 6842; fax: +81 726 0731.
E-mail address: takiyama@eng.hokudai.ac.jp (T. Akiyama).
[1] Graduate student, Hokkaido University.

0925-8388/$ – see front matter © 2009 Elsevier B.V. All rights reserved.
doi:10.1016/j.jallcom.2009.08.094

The MASHS process, which was originally proposed by Gaffet and Bernard [13–15], is the combination of the two phases (MA and SHS). The first phase is that raw materials are mechanically activated by kinetic energy, such as frequent shocks, caused by high-energy ball milling (HBM). In general, a planetary ball mill (PBM) is the most widely used in laboratories, in which the milling pot, being horizontally fixed onto a rotating disc, rotates in the opposite direction to the disk. In the second phase, the MA sample is ignited by an external heat source for self-propagating exothermic reaction to provide the desired product without any additional energy; the SHS process utilizes exothermic chemical reaction efficiently between metallic powders and an oxidant of the reactants. Several reports revealed that the MA was of help to sustain a combustion front in SHS systems with the weak exothermic reaction, e.g. Fe–Si [16] and Cu–Si [17]. Also, the MASHS was applied to produce nanostructured intermetallic compounds of FeAl [18,19] and $NbAl_3$ [20,21] with success. However, the MASHS of LSGM9182 has never been reported so far in spite of its engineering importance. In contrast, only HBM process without SHS, based on so-called mechanochemical reaction, was employed to synthesize many functional perovskite-type oxides: e.g. $LaMnO_3$ [22], $LaGaO_3$ [23], $La_{0.7}Sr_{0.3}MnO_3$ [24] and $La_{1-x}Sr_xFeO_{3-\delta}$ [25].

Therefore, the purpose of this paper is to synthesize highly pure LSGM9182 powder with high crystallinity by the MASHS; the effect of milling time in the MA process using the PBM on the starting materials for the LSGM9182 production was experimentally investigated. Also, the synergy effect of the MA treatment and the SHS was examined by comparing to the only SHS.

2. Experimental

Raw materials for MASHS of LSGM9182 selected were the same ones used in the previous SHS [4,5]: i.e. La_2O_3 and $SrCO_3$ (Aldrich, 99.9% in purity), Ga_2O_3 and Mg (Kojundo Chemical, 99.9% in purity) and $NaClO_4$ (Aldrich, 98% in purity). These commercially available powders were stoichiometrically mixed as the starting mixture for the planetary ball milling (PBM, Fritsch, P-6). In the MA treatment, PBM was performed at a rotation speed of 300 rpm under atmospheric condition. The starting mixture was co-milled with stainless-steel (SUS303) balls of 10 mm in diameter into a stainless-steel pot for different periods, in which the mass ratio of ball-to-powder was fixed at 10/1. The mixing method of the previous SHS without the PBM is described elsewhere [4,5]. After the PBM process, the sample of 3 g per test was pressed into a disk of 20 mm in diameter at 50 MPa using a uniaxial single-acting press.

The SHS procedure is as follows; at the beginning, the green compact of the MA sample was placed into a graphite crucible, and a disposable carbon foil as an igniter was also set in contact with the bottom surface of the sample. Secondly, argon (99.99 mol%) of atmospheric pressure was supplied to the SHS reactor after being evacuated by a rotary pump for 10 min. Finally, the igniter was electrically heated at room temperature to propagate a combustion wave continuously. All the phenomena of ignition, propagation and completion during the SHS were observable through the upper glass window of the apparatus. The SHSed product was poured into ion-exchange water and washed by an ultrasonic cleaner to remove solid sodium chloride from the sample.

All of the products were characterized by X-ray diffraction (XRD, JDX-3500, JEOL) analyzer to qualitatively identify the possible phase, and evaluated by the particle size analyzer (LA-920, Horiba). Microstructure of the sample was also observed by Field-Emission Scanning Electron Microscopy (FESEM, JSM-6500F, JEOL). The powder surface was sputter coated with graphite before the SEM analysis. The results of measurement were evaluated comparatively with the previous SHSed sample without the MA treatment. In addition, contamination of the samples, which might come from the stainless-steel pot and balls during the PBM, was quantitatively estimated by X-ray Fluorescence (XRF, μEDX-1200, Shimadzu) analysis with possible measurements from Al to U. Specific surface area of the powder obtained was also measured by nitrogen gas adsorption equipment (BELSORP-mini, Bel Japan) based on the BET method.

3. Results and discussion

3.1. Effect of mechanical activation on starting materials for LSGM9182

Fig. 1 shows XRD patterns of raw materials after the PBM process for different periods. The reference data of starting materials without the MA treatment is also given here. Obviously, the amorphous phase increased with increasing milling time, that is, the peak strength lowered and the peak width broadened. Consequently, after the PBM for as much as 24 h, the crystalline reactants transformed into the amorphous state completely. During the PBM, the raw materials were mechanically activated due to the disordering of crystal lattice by kinetic energy; this means so-called atomic mixture on angstrom scale. This is probably because that thermal and strain energy, generated during the PBM, distorted the orderly crystal lattice within the raw materials.

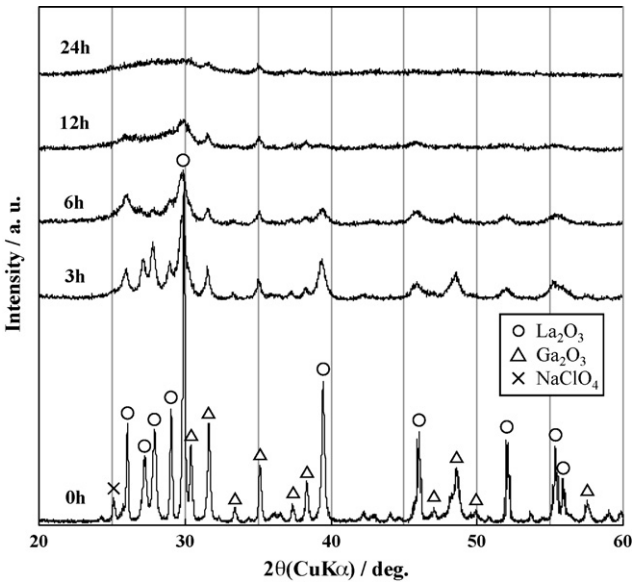

Fig. 1. XRD patterns of raw materials after planetary ball milling for different periods. The reference data of the starting materials without the MA treatment is also shown.

Much care was paid to contamination from the stainless-steel pot or balls used for the PBM; the MA sample was quantitatively estimated by XRF analysis. Table 1 gives mass fraction of the components contained in the starting mixture after the PBM for 24 h. Here, each element of theoretical mass fraction was calculated from desired mixing ratio of raw materials. It was confirmed that data of theoretical and experimental one has the similar tendency, except soda. The trace elements of Zr (0.14 mass%) and Fe (0.061 mass%) were rather detected except the major elements of raw materials; the lightweight metals of Mg and Na were not suitably detected. The impurities of Zr and Fe in the MA sample were less than 0.01 mol% at the conversion into the molar ratio. Therefore, we judged the contamination from milling pot and balls have no significant effect on the final product because the amount of impurities was vanishingly small.

Fig. 2(a) gives particle size distributions of raw materials after the PBM for various milling periods; moreover, change in the aver-

Table 1
Mass fraction of components contained in the starting mixture with planetary ball milling for 24 h by XRF analysis.

Element	Theoretical mass fraction/mass%	Experimental mass fraction/mass%
La	58.2	59.1
Ga	29.8	27.1
Sr	5.85	4.01
Cl	4.25	9.55
Mg	1.93	–
Zr	–	0.140
Fe	–	0.0607

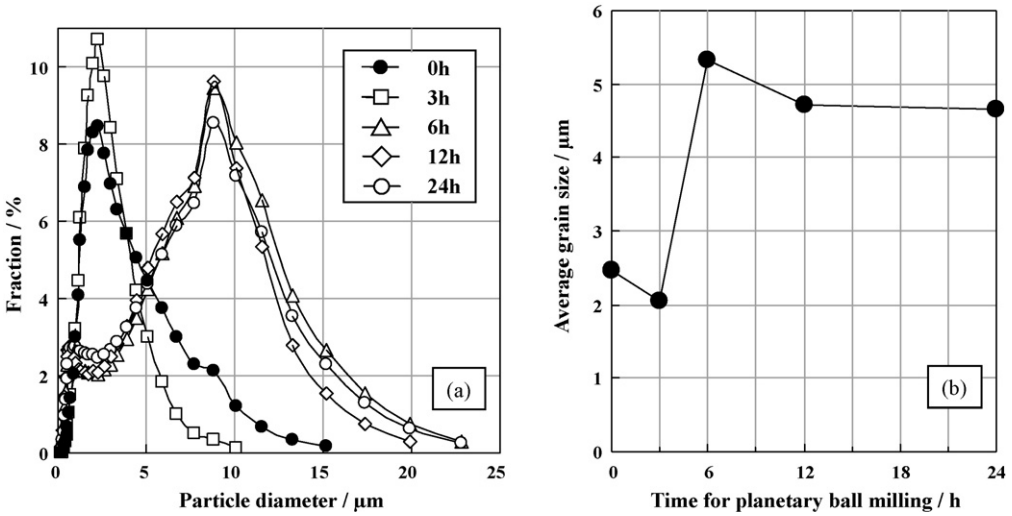

Fig. 2. (a) Particle size distributions of raw materials after planetary ball milling for various time intervals and (b) change in the average grain size with time for planetary ball milling.

age grain size with time for the PBM is also shown in Fig. 2(b). The MA sample with the PBM of 3 h had higher peak in 2 μm, a reduced curve over 2 μm and smaller average particle size in comparison to that of 0 h, because of grinding of the coarse grains over 5 μm. However, the long time PBM brought unexpected results; that is, over 3 h in the PBM, the average particle size did not decrease but increased notably and reached almost constant value, 5 ± 0.4 μm.

Fig. 3 gives SEM micrographs of the raw materials with the PBM of 24 h, in comparison to that of no PBM. In appearance, the difference between the starting materials with/without the MA treatment emerged clearly; the photograph (a) shows an agglomerate powder consisting of fine primary particles with size of less than 100 nm, while photograph (b), a typical smooth surface of the reactant. The agglomeration between the particles during the MA treatment can be easily explained as follows. In the initial stage of MA process less than 3 h, stress given in the PBM process flattened the ductile metallic Mg, while fragmenting the brittle components such as La_2O_3, $SrCO_3$, Ga_2O_3 and $NaClO_4$. After both flattening and fracturing, the coalescence of the particles occurred with increasing milling time from 3 h to 6 h. From the results of the particle size distribution, it seems that the PBM longer than 3 h led to the active coalescence between the grains. Indeed, the sample color distinctly turned from white to light gray in appearance after the PBM for 24 h. In conclusion, the paramount cause of the larger particle size was due to the active agglomeration between the particles of reactants with longer milling.

3.2. Characterization of MASHSed LSGM9182 powders

In our previous reports, the conventional SHS process of LSGM9182 did not go through despite the ignition due to weak exothermic heat caused by oxidative reaction of small amount of magnesium [4,5]. In contrast, the MA treatment employed in this study improved a reactivity of the SHS for synthesizing the LSGM9182 very drastically, in which the following exothermic reaction proceeded for producing the LSGM9182:

$$0.45La_2O_3 + 0.1SrCO_3 + 0.4Ga_2O_3 + 0.2Mg + 0.0875NaClO_4 \rightarrow La_{0.9}Sr_{0.1}Ga_{0.8}Mg_{0.2}O_{3-\delta} + 0.1CO_2(g) + 0.0875NaCl(g) \quad (1)$$

Any green compact after the MA process ignited successfully, the reaction front propagated continuously with the propagation rate of approximately 0.2 g/s, and the SHS process went through. Also, the MASHSed samples, in particular the product with the PBM

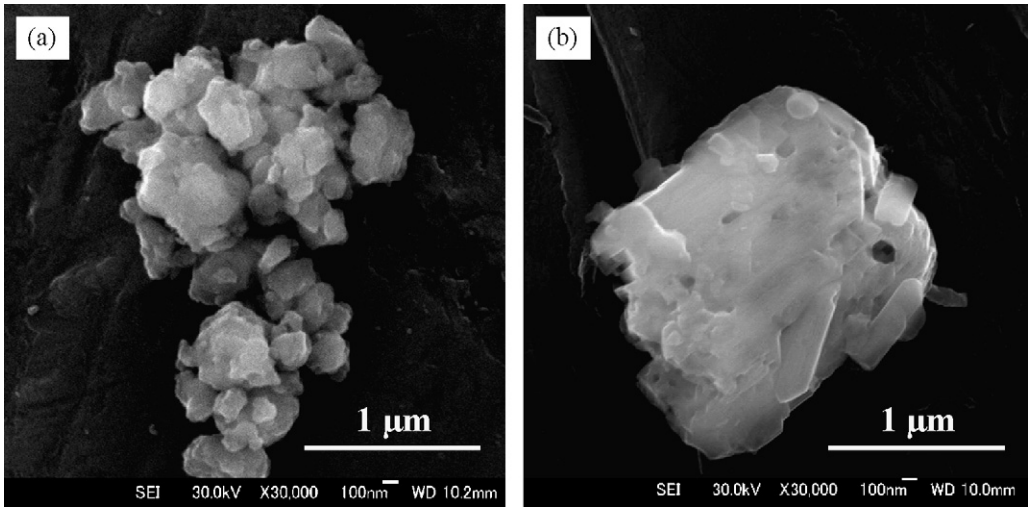

Fig. 3. SEM micrographs of the raw materials; (a) with planetary ball milling for 24 h and (b) without planetary ball milling.

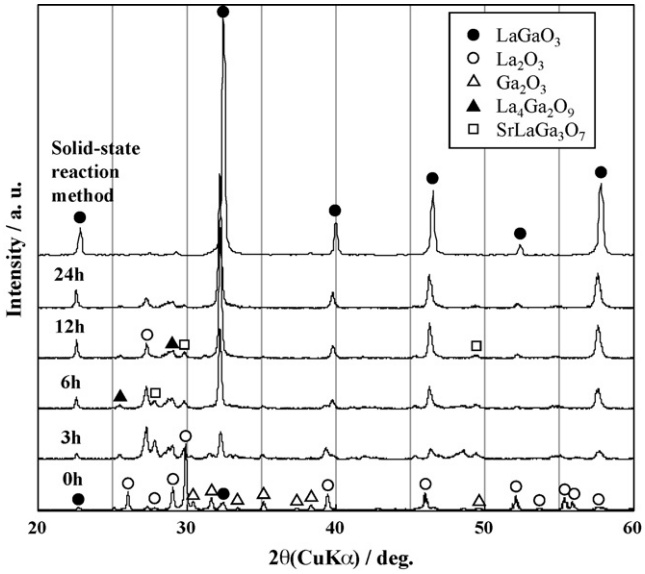

Fig. 4. XRD patterns of the MASHS-samples after planetary ball milling for different periods. The reference data of the products by the previous SHS and the solid-state reaction method are shown as well.

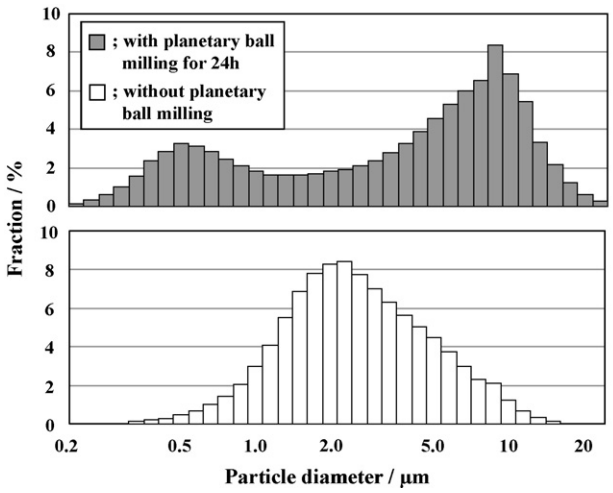

Fig. 5. Comparison of particle size distribution between the SHSed products with/without planetary ball milling for 24 h as pretreatment.

for 24 h, had cream in color, and rough shape and very porous in surface, as mentioned later.

Fig. 4 shows changes in XRD pattern for the SHSed products with the PBM process of different periods. Here, the reference data of the LSGM9182 samples by the conventional SHS and SRM are also given. Obviously, the peak strength of the aimed perovskite phase ($LaGaO_3$) in the product increased with longer milling; in contrast, that of the un-reacted La_2O_3 and Ga_2O_3 and secondary phases, such as $La_4Ga_2O_9$ and $SrLaGa_3O_7$, decreased gradually. Significantly, the MASHS for 24 h synthesized the LSGM9182, lattice parameters of which were $a = 5.537$ Å, $b = 5.546$ Å and $c = 7.858$ Å. They agreed well with the reference values of JCPDS card: $a = 5.515$ Å, $b = 5.539$ Å and $c = 7.816$ Å. The distinct difference between the MASHSed and the SHSed products of LSGM9182 means the improvement of the SHS reactivity thanks to the MA pretreatment, which was caused by the two facts: (1) the contact area between the raw materials was enlarged by flattening the ductile Mg and fracturing the brittle oxides and carbonate during the MA process, and (2) the lattice energy in the reactants was accumulated due to the crystal structure distortion from kinetic energy of the PBM.

Table 2
Mass fraction of components contained in the MASHSed product with planetary ball milling for 24 h by XRF analysis.

Element	Theoretical mass fraction/mass%	Experimental mass fraction/mass%
La	64.3	64.4
Ga	28.7	30.6
Sr	4.51	4.60
Mg	2.01	–
Zr	–	0.248
Fe	–	0.218

Table 2 gives mass fraction of components contained in the MASHSed product with the PBM of 24 h according to XRF analysis. Here, the lightweight metal of Mg was not detected, as expected. The measured mass fraction of La, Ga and Sr elements almost corresponded to the theoretical value. In other words, the product agreed well with stoichiometric compound of LSGM9182. Note, however, that the trace amount of Zr (0.248 mass%) and Fe (0.218 mass%) was also detected as contamination, which was comparable to approximately 1.3 mol%. Probably, this came from the milling pot and balls during the MA treatment, but the amount was of no significance. Therefore, we confirmed that the MASHS with the PBM of 24 h successfully synthesized the LSGM9182 product at aimed ratios.

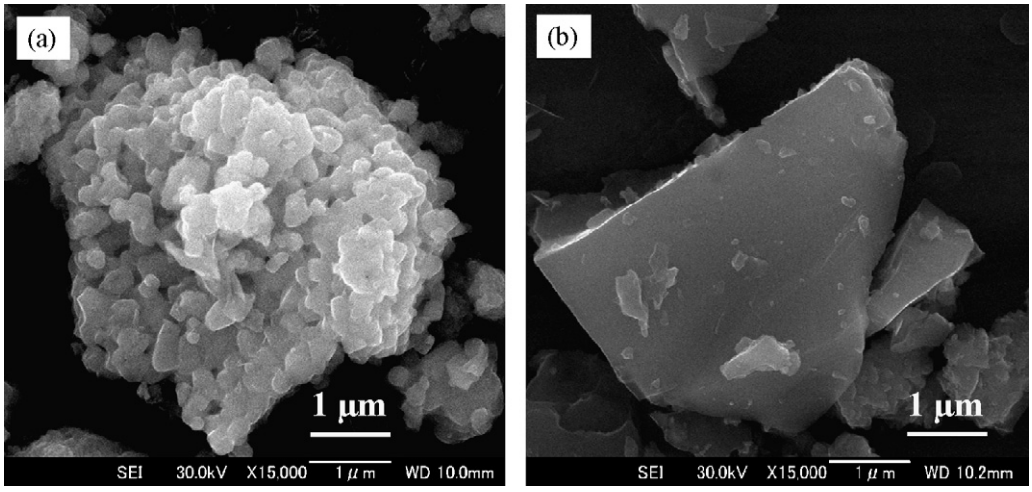

Fig. 6. SEM micrographs of the $La_{0.9}Sr_{0.1}Ga_{0.8}Mg_{0.2}O_{3-\delta}$ (LSGM9182) particles; (a) after MASHS, planetary ball milling for 24 h, and (b) after SHS without the MA treatment.

Fig. 5 shows comparison of the particle size distribution between the SHSed products with/without the PBM of 24 h. The fine LSGM9182 powder with submicron size was rather obtained, while the coarse particles larger than 5 μm in size were increased as well; this tendency was similar to the particle size distribution of the raw materials after the PBM for 24 h (see Fig. 2(a)). In addition, the grain size of the MASHSed product was 4.6 μm in average, larger than the conventional SHSed product, 2.3 μm. The results were apparently due to the agglomeration of the reactants by the PBM. It suggested that the prevention of its agglomeration is a key factor for obtaining the finer and monodisperse LSGM9182 powders in the MASHS.

Fig. 6 gives the SEM micrographs of the LSGM9182 particles both after MASHS with the PBM of 24 h and after the previous SHS without the PBM. Evidently, the microstructure of the MASHSed powder was different from the particle surface by the conventional SHS, which was the aggregate of the fine primary particles in nano-size. Note that nano-pores from evaporation of NaCl and CO_2 during the reaction were precisely observed as well. Moreover, the specific surface area (S_{sp}) of the MASHSed product for 24 h was 3.36 m^2/g in spite of the relative large particles, much higher than the value by the previous SHS (S_{sp} = 2.06 m^2/g). Therefore, the MASHS for 24 h led to the high-grade LSGM9182 powders with the nano-sized primary particles and the large specific surface area.

4. Conclusion

The combination of MA and SHS was highly effective for the production of LSGM9182. This can be widely applied to general SHS systems of weak exothermic reaction. The detailed conclusions were:

(1) In the MA process using the planetary ball mill, the crystal lattice of the raw materials gradually became disordered, i.e. amorphous state, with increasing the milling time, and the crystalline reactants of La_2O_3, $SrCO_3$, Ga_2O_3, Mg and $NaClO_4$ entirely turned into the amorphous phase in 24 h. With increasing the milling time, average particle size of the raw materials increased, not decreased, in which nanoparticles, generated by milling, became massed together.

(2) In the SHS process with the MA treatment of the raw materials, the reactivity for the LSGM9182 production was drastically improved, in which all of the products had much more rich perovskite-type oxide, in comparison to only SHS process. The MA treatment with longer milling time was effective for purifying the final product. The 24 h in the milling time made the highest-grade LSGM9182 powder with high crystallinity, purity of which was almost the same as one in the conventional solid-state reaction method. Moreover, the final product was porous, being agglomerated by the nano-sized primary particles.

The results appealed a new possibility of the MASHS for synthesizing versatile functional perovskite-type materials. The porous and nano-sized ceramics powder obtained by the MASHS must have wide industrial applications such as a catalyst.

Acknowledgements

This research was partially supported by the national project "*Demonstration of Green-Hydrogen Community in Honjo-Waseda area*", Ministry of the Environment, Japan.

The authors are most grateful to Prof. T. MASUDA and Dr. T. TAGO, *Division of Chemical Engineering*, *Graduate School of Engineering*, *Hokkaido University*, for kindly allowing us to use the measuring instrument for specific surface area.

References

[1] T. Ishihara, H. Matsuda, Y. Takita, J. Am. Chem. Soc. 116 (1994) 3801.
[2] T. Ishihara, H. Matsuda, Y. Takita, Solid State Ionics 79 (1995) 147.
[3] M. Feng, J.B. Goodenough, Eur. J. Solid State Inorg. Chem. T31 (1994) 663.
[4] H. Ishikawa, M. Enoki, T. Ishihara, T. Akiyama, Mater. Trans. 47 (2006) 149.
[5] H. Ishikawa, M. Enoki, T. Ishihara, T. Akiyama, Int. J. SHS 15 (2006) 1.
[6] K. Kuroda, I. Hashimoto, K. Adachi, J. Akikusa, Y. Tamou, N. Komada, T. Ishihara, Y. Takita, Solid State Ionics 132 (2000) 199.
[7] J. Akikusa, K. Adachi, K. Hoshino, T. Ishihara, Y. Takita, J. Electrochem. Soc. 148 (2001) A1275.
[8] K.Q. Huang, J.B. Goodenough, J. Solid State Chem. 136 (1998) 274.
[9] O. Schulz, M. Martin, Solid State Ionics 135 (2000) 549.
[10] J.W. Stevenson, T.R. Armstrong, L.R. Pederson, J. Li, C.A. Lewinsohn, S. Baskaran, Solid State Ionics 113–115 (1998) 571.
[11] J.W. Stevenson, K. Hasinska, N.L. Canfield, T.R. Armstrong, J. Electrochem. Soc. 147 (2000) 3213.
[12] L.G. Cong, T.M. He, Y. Ji, P.F. Guan, Y.L. Huang, W.H. Su, J. Alloys Compd. 348 (2003) 325.
[13] E. Gaffet, F. Charlot, F. Bernard, D. Klein, J.C. Niepce, Mater. Sci. Forum 269–272 (1998) 379.
[14] F. Bernard, F. Charlot, E. Gaffet, J.C. Niepce, Int. J. SHS 7 (1998) 233.
[15] F. Bernard, E. Gaffet, Int. J. SHS 10 (2001) 109.
[16] Ch. Gras, E. Gaffet, F. Bernard, J.C. Niepce, Mater. Sci. Eng. A264 (1999) 94.
[17] F. Bernard, H. Souha, E. Gaffet, Mater. Sci. Eng. A284 (2000) 301.
[18] F. Charlot, E. Gaffet, B. Zeghmati, F. Bernard, J.C. Niepce, Mater. Sci. Eng. A262 (1999) 279.
[19] F. Charlot, F. Bernard, E. Gaffet, D. Klein, J.C. Niepce, Acta Mater. 47 (1999) 619.
[20] V. Gauthier, C. Josse, F. Bernard, E. Gaffet, J.P. Larpin, Mater. Sci. Eng. A265 (1999) 117.
[21] V. Gauthier, F. Bernard, E. Gaffet, D. Vrel, M. Gailhanou, J.P. Larpin, Intermetallics 10 (2002) 377.
[22] Q. Zhang, F. Saito, J. Alloys Compd. 297 (2000) 99.
[23] Q. Zhang, J. Lu, J. Wang, F. Saito, J. Mater. Sci. 39 (2004) 5527.
[24] Q. Zhang, T. Nakagawa, F. Saito, J. Alloys Compd. 308 (2000) 121.
[25] I.S. Yakovleva, L.A. Isupova, S.V. Tsybulya, A.V. Chernysh, N.N. Boldyreva, G.M. Alikina, V.A. Sadykov, J. Mater. Sci. 39 (2004) 5517.